Global Journal of Researches in Engineering: a
Mechanical and Mechanics Engineering
Volume 17 Issue 5 Version 1.0 Year 2017
Type: Double Blind Peer Reviewed International Research Journal
Publisher: Global Journals Inc. (USA)
Online ISSN:2249-4596 Print ISSN:0975-5861

First and Second Laws Analysis and Optimization of a Solar Absorber; Using Insulator Mixers and MWCNTs Nanoparticles

By Soroush Sadripour
University of Kashan

Abstract- In this paper, forced convection flow and heat transfer of MWCNTs-water nanofluid in heat sink collector equipped with mixers are studied. The three-dimensional governing equations are numerically solved in the domain by the control volume approach based on the SIMPLE algorithm. Reynolds numbers are considered in laminar-turbulent range of $50<Re<12,000$. The optimization was carried out by comparison of different parameters to reach the optimal case with the maximum exergy efficiency. From this study, it is concluded that in the case of using heat sink, instead of shell and tubes, the time that the fluid is inside the collector increases and leads to outlet temperature increase from the collector the exergy efficiency increases. Also, it is realized that using mixers enhance the outlet fluid temperature, energy efficiency and exergy efficiency.

Keywords: *heat sink collector, exergy optimization, radiation, forced convection, mixer, MWCNTS.*

GJRE-A Classification: *FOR Code: 850599*

Strictly as per the compliance and regulations of:

First and Second Laws Analysis and Optimization of a Solar Absorber; Using Insulator Mixers and MWCNTs Nanoparticles

Soroush Sadripour

Abstract- In this paper, forced convection flow and heat transfer of MWCNTs-water nanofluid in heat sink collector equipped with mixers are studied. The three-dimensional governing equations are numerically solved in the domain by the control volume approach based on the SIMPLE algorithm. Reynolds numbers are considered in laminar-turbulent range of 50<Re<12,000. The optimization was carried out by comparison of different parameters to reach the optimal case with the maximum exergy efficiency. From this study, it is concluded that in the case of using heat sink, instead of shell and tubes, the time that the fluid is inside the collector increases and leads to outlet temperature increase from the collector the exergy efficiency increases. Also, it is realized that using mixers enhance the outlet fluid temperature, energy efficiency and exergy efficiency. Generally, while the trend of exergy efficiency variation with effective parameters is increasing, applying the mixers precipitate the efficiency increment. In addition, for the case that the trend of exergy efficiency variation with changing these parameters is decreasing, the decreasing trend gets slow. Finally, the highest exergy efficiency was obtained for the nanoparticle volume fraction of ϕ=0.10%.

Keywords: heat sink collector, exergy optimization, radiation, forced convection, mixer, MWCNTS.

I. Introduction

The use of solar energy offers numerous advantages, especially in Iran where levels of radiation from the sun are much higher than average and where many provinces lack any centralized infrastructure to support a national energy supply. While the demand for energy rapidly increases in Iran, using the necessary technology for converting energy from the sun's rays into useful energy is much important for the vast majority of the population [1]. Solar energy has a remarkably higher potential compared to other renewables energy, such as wind, ocean, hydro, biomass and geothermal. There are many types of systems that employ solar energy collectors as a source of input energy to drive a process. Between these all systems the flat-plate solar collector comparing with other collector types has simple design and low costs of construction. In addition to direct solar radiation absorption they can also absorb the diffuse radiation [2]. So far a lot of numerical and empirical studies related to solar collectors have been conducted. The results of these studies demonstrate that the overall performance of collector is related to many factors including the distance between absorber plate and glass cover and pipe diameter [3, 4], wind velocity [5], solar radiation [6], collector material [7], flow rate [8], and channel depth [9]. But one proper solution to improve the efficiency of solar collectors is to use heat sink below the absorber plate instead of pipes. It can increase the wetted surface between fluid and absorber, and also increase outlet temperature of fluid. Furthermore, employing mixers in the heat exchangers has been one of the frequent approaches to break the laminar sub-layer and create local turbulence due to flow separation and reattachment between successive obstacles, which reduces the thermal resistance and significantly enhances the heat transfer [10]. This paper focuses on energy analysis of heat sink flat plate solar collector equipped with mixers for enhancing the thermal performance and the maximum energy efficiency and exergy efficiency under given operating conditions. Another method is to increase the heat transfer between fluid and solar absorbing plate. One common and suggested way is to add the nanoparticles to the base fluid used in collector.

Baniamerianand et al. [11] studied numerically aerodynamic coefficients of solar troughs considering terrain effects and vortex shedding. Their results show that in order to properly align trough collector in solar farms, it is essential to study the vortices shed created at the behind of parabolic troughs. In another numerical investigation Ziapour and Rahimi [12] investigated natural convection heat transfer in a horizontal wavy absorber solar collector based on the second law analysis. Their results show that with increasing of the cosine wave amplitude, the collector enclosure irreversibility decreases. Ajay and Kundan [13] studied performance evaluation of nanofluid (Al_2O_3/H_2O-$C_2H_6O_2$) based parabolic solar collector using both experimental and CFD techniques. Their results show a close agreement between experimental and CFD result.

A method for establishing the optimal operation mode of solar collectors derives from the exergy analysis of the processes specific for the fluid that passes through the collector's stream tube [14]. The

Author: Department of Mechanical Engineering, University of Kashan, Iran. e-mail: soroushsadripour@hotmail.com

analyzed relevant literature contains studies on the dependence of the exergy efficiency on the fluid flow rate and on the fluid temperature at the entrance into the collector serpentine pipe. The specific exergy of the fluid in the solar collector as depending on the inlet temperature, the parameter being either the solar radiation or the fluid flow rate, presents points of local maximal. These aspects are not highlighted in the energy efficiency equation. Shojaeizadeh and Veysi [15] developed a correlation for parameter controlling exergy efficiency optimization of an Al2O3/water nanofluid based flat-plate solar collector. Said et al. [16] investigated energy and exergy analysis of a flat-plate solar collector using different sizes of Aluminum oxide based nanofluid and they founded that the combination of energy and exergy analysis is an appropriate method to optimize the flat-plate solar collectors.

Mollamahdi et al. [17] investigated flow field and heat transfer in a channel with a permeable wall filled with Al_2O_3-Cu/water micropolar hybrid nanofluid, effects of chemical reaction and magnetic field. Their results show that with increasing the Hartmann number and the Reynolds number, the Nusselt and Sherwood numbers increase. Furthermore, when the hybrid nanofluid is applied rather than pure nanofluid, the heat transfer coefficient will increase significantly. Hemmat Esfe and Saedodin [18] studied numerically of combined convection flow in a cavity subjected to a nanofluid with an inside hot obstacle: effect of diameter of nanoparticles and cavity inclination angles. Their obtained results show that the average Nusselt number for all range of solid volume fraction decreases with increase in diameter of nanoparticles

The literature review elucidates that although usage of stationary obstacle to investigate the efficiency of heat sink flat-plate air heaters has been assessed, but to the best of author's knowledge there is not any study which investigates effect of using mixers and Multi Wall Carbon Nano Tubes (MWCNTs) nanoparticles in water based heat sink solar collectors on the first and second law efficiencies of solar collectors. Therefore, this study is expected to fulfill the research gap about usage of insulator mixers in heat sink solar collector using nanofluid. The other objective of this study is to investigate the effect of different suspended nanoparticles volume fractions on the energy and exergy efficiencies of water based MWCNTs nanofluids numerically using finite volume method.

II. Methodology

a) Physical Model

The three-dimensional schematic diagram of heat sink of a flat-plate solar collector equipped with mixers is shown in "Fig. 1". "Table 1" represents different properties of this heat sink collector. For simulation, useful received energy by collector is calculated based on inlet solar radiation and overall heat loss by analytical relations. Then the three-dimensional heat sink collector investigates numerically and useful received energy by fluid, outlet temperature of fluid and energy and exergy efficiencies obtained. The flow inside the channel is considered steady and turbulent. For the inlet section of the sink the velocity inlet boundary condition in is considered and for the outlet section of the heat sink pressure outlet boundary condition is assumed. The absorber plate is produced from Aluminum with matted black color and is under the uniform heat flux that is calculated with assuming optical properties and overall heat loss of collector for different sunny hours based on empirical measurements results of Khorasanizadeh et al. [2] for a reference collector in Tehran located in Iran ("Table 2"). Due to simulating mixers assumptions with no slip condition are considered. Also, all of these obstacles with diameter of D_o are insulator. Because of considering influences of overall heat loss in calculating of useful received energy by collector other walls of heat sink are assumed insulator.

Table 1: Properties of collectors simulated in present study

Properties	Symbo	Value
Dimensions of collector	$L_c \times W_c$ (mm)	200×92.5
Dimensions of inlet section	$L_i \times W_i$ (mm)	10×20
Dimensions of exit section	$L_e \times W_e$ (mm)	10×20
Height of heat sink	H (mm)	1.5
Slop of collector	B	35°
Number of glass covers	N	1
Emissivity of glass covers	ε_g	0.85
Thickness of plate	δ_p (mm)	0.1
Emissivity of plate	ε_p	0.9
Conductivity of plate	k_p (W·m^{-1}·K^{-1})	211
Optical efficiency	η_0	0.68
Thickness of insulators	δ_{ins} (mm)	2.0
Conductivity of insulators	k_{ins} (W·m^{-1}·K^{-1})	0.05
Number of mixers	n_o	3
Location of first mixer	L_{fo} (mm)	38
Location of other mixers	L_o (*mm*)	50
Diameter of mixers	D_o (mm)	0.5

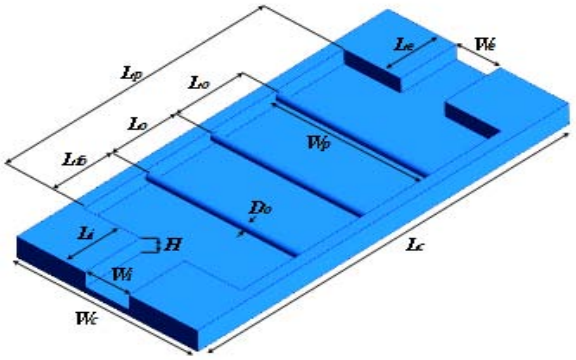

Figure 1: Schematic diagram of the heat sink of a flat plate solar collector equipped with mixers

Table 2: Empirical results of Khorasanizadeh et al. [2] for reference collector installed in Tehran

Time	I_T (W·m^{-2})	T_a (°C)	T_{in} (°C)	V_w (m·s^{-1})
09:00	560	33	44.5	6
09:30	630	33	45	6
10:00	750	34	46	5
10:30	830	35	47	6
11:00	925	36	50	6
11:30	992	37	51	5
12:00	1006	38	53	5
12:30	1020	38.5	54	6
13:00	978	40.5	56	6
13:30	914	40.5	57	5
14:00	834	41	60	5
14:30	780	41	61	4
15:00	734	39.5	62	5
15:30	626	41	63	6
16:00	607	41	64	6

b) Governing Equations

The governing equations for flow and heat transfer in the flat-plate solar collector can be written in the Cartesian tensor system as [19]:

$$\frac{\partial}{\partial x_i}(\rho u_i) = 0 \tag{1}$$

$$\frac{\partial}{\partial x_j}(\rho u_i u_j) = -\frac{\partial P}{\partial x_j} + \frac{\partial}{\partial x_j}\left[\mu\left(\frac{\partial u_i}{\partial x_j} + \frac{\partial u_j}{\partial x_i}\right)\right] + \frac{\partial}{\partial x_j}\left(-\rho\overline{u_i' u_j'}\right) \tag{2}$$

$$\frac{\partial}{\partial x_i}(\rho u_i T) = \frac{\partial}{\partial x_j}\left[\left(\frac{\mu}{\mathrm{Pr}} + \frac{\mu_t}{\mathrm{Pr}_t}\right)\frac{\partial T}{\partial x_j}\right] \tag{3}$$

where ρ is the density of fluid and u_i is the axial velocity, μ, $\acute{u}$ and u_j are the fluid viscosity, fluctuated velocity and the axial velocity, respectively, and the term $\rho\overline{u_i' u_j'}$ is the turbulent shear stress. The Reynolds averaged approach to turbulence modelling requires that the Reynolds stresses $\rho\overline{u_i' u_j'}$ in "Eq. 2" needs to be modelled. For closure of the equations, the *k-ε* turbulence model was chosen. A common method employs the Boussinesq hypothesis to relate the Reynolds stresses to the mean velocity gradient:

$$-\rho\overline{u_i' u_j'} = \mu_t\left(\frac{\partial u_i}{\partial x_j} + \frac{\partial u_j}{\partial x_i}\right) \tag{4}$$

The turbulent viscosity term μ_t is to be computed from an appropriate turbulence model. The expression for the turbulent viscosity is given as "Eq. 5". In the equation of the TKE, *k* is written as "Eq. 6".

$$\mu_t = \rho C_\mu \frac{k^2}{\varepsilon} \tag{5}$$

$$\frac{\partial}{\partial x_i}\left[\rho k u_i\right] = \frac{\partial}{\partial x_j}\left[\left(\mu + \frac{\mu_t}{\sigma_k}\right)\frac{\partial k}{\partial x_j}\right] + G_k - \rho\varepsilon \tag{6}$$

Similarly, in the dissipation rate of TKE, ε is given by the following equation:

$$\frac{\partial}{\partial x_i}\left[\rho\varepsilon u_i\right] = \frac{\partial}{\partial x_j}\left[\left(\mu + \frac{\mu_t}{\sigma_\varepsilon}\right)\frac{\partial \varepsilon}{\partial x_j}\right] + C_{1\varepsilon}\frac{\varepsilon}{k}G_k + C_{1\varepsilon}\rho\frac{\varepsilon^2}{k} \tag{7}$$

where G_k is the rate of generation of the TKE while $\rho\varepsilon$ is its destruction rate, G_k is written as:

$$G_k = -\rho\overline{u_i' u_j'}\frac{\partial u_j}{\partial x_i} \tag{8}$$

The boundary values for the turbulent quantities near the wall are specified with the enhanced wall treatment method. C_μ=0.09, $C_{1\varepsilon}$=1.44, $C_{2\varepsilon}$=1.92, σ_k=1.00, σ_ε=1.30 and Pr_t=0.90 are chosen to empirical constants in the turbulence transport equations [19].

The fluid is considered to be Newtonian, and the physical properties of the fluid are temperature dependent. Since the temperature variations is higher than 3°C [20]. The following polynomial expansions are used [21]:

$$\rho(T) = 5.3738\cdot10^{-10}T^5 - 9.59976\cdot10^{-7}T^4 + 6.93809\cdot10^{-4}T^3 - 0.255822T^2 + 47.8074T - 2584.53 \tag{9}$$

$$c_p(T) = -4.51782\cdot10^{-8}T^5 + 7.61613\cdot10^{-5}T^4 - 5.12699\cdot10^{-2}T^3 + 17.2363T^2 - 2894.85T + 198532 \tag{10}$$

$$k(T) = 5.15307 \cdot 10^{-11} T^5 - 8.15212 \cdot 10^{-8} T^4 + 5.138 \cdot 10^{-5} T^3 - 1.61344 \cdot 10^{-2} T^2 + 2.52691 T - 157.532 \quad (11)$$

$$\mu(T) = -4.37087 \cdot 10^{-13} T^5 + 7.38482 \cdot 10^{-10} T^4 - 4.99292 \cdot 10^{-7} T^3 + 1.68946 \cdot 10^{-4} T^2 - 2.86313 \cdot 10^{-2} T + 1.94641 \quad (12)$$

The spectral radiative transfer equation (RTE) can be written as "Eq. 13".

$$\frac{dI_v(r,s)}{ds} = -(K_{av} + K_{sv}) I_v(r,s) + K_{av} I_b(v,T) + \frac{K_{sv}}{4\pi} \int_{4\pi} dI_v(r,s') \cdot \phi(s.s') d\Omega' + S \quad (13)$$

where I_v is spectral radiation intensity which depends on position r and direction s. [22]:

$$I_v(r,s) = \varepsilon_v(r_w) I_b(v,T) + \frac{\rho_w(r_w)}{\pi} \int_{n.s'<0} I_v(r,s') \cdot |n.s'| d\Omega' \quad (14)$$

The commercial available CFD software, FLUENT 15.0 was used to solve the governing equations. The control volume approach was used to solve the system of classical single phase governing equations by using the finite volume method (FVM). The standard k–ε turbulence model with enhanced wall function was selected. The diffusion term in the momentum and energy equations was approximated by second-order central difference. In addition, a second-order upwind differencing scheme was adopted for the convective terms.

The convergence criterion was considered 10^{-6} for all variables.

c) First law modeling

Useful received energy by fluid in collector is calculated as follow [23]:

$$\dot{Q}_{u,f} = \dot{m}_f \cdot c_p (T_{out} - T_{in}) \quad (15)$$

where $\dot{m}_f$ is mass flow rate of fluid, c_p is specific heat capacity of fluid and T_{in} and T_{out} are mean temperature of inlet and outlet fluid, respectively.

Useful received energy by collector based on inlet solar radiation and overall heat loss is as follow:

$$\dot{Q}_{u,c} = A_c \left[S - U_L (T_{pm} - T_a) \right] \quad (16)$$

where A_c is the area of absorber plate, T_a is ambient temperature and T_{pm} is mean temperature of absorber plate. It should be noticed that the temperature of absorber plate is not a constant value and considering a mean temperature for it just is a virtual concept.

In the present study temperature gradients around heat sink can be neglected and a mean temperature can be taken into account for it as far as heat sink has been spread through the absorber plate, and also the thermal conductivity of welding between plate and sink, thermal conductivity of plate and the convection heat transfer coefficient of fluid are high.

Also in "Eq. 16", S is a part of solar radiation per plate area unit that is absorbed by absorber plate and is as follow:

$$S = \eta_0 \cdot I_T \quad (17)$$

where I_T is daily average hourly radiation entered to collector and η_0 is optical efficiency of collector and is calculated as follow:

$$\eta_0 = (\tau\alpha) = 1.01 \tau \cdot \alpha \quad (18)$$

Also, I_T is calculated as follow:

$$I_T = I_b R_b + I_d \left[\frac{1+\cos\beta}{2} \right] + I \cdot \rho_{gr} \left[\frac{1-\cos\beta}{2} \right] \quad (19)$$

where I, I_b and I_d are solar radiation on horizontal surface, beam radiation and diffuse radiation, respectively.

Also, R_b is ratio of beam radiation on tilted surface to that on horizontal surface and is calculated as follow:

$$R_b = \frac{\cos(\varphi-\beta)\cos\delta\cos(\omega) + \sin(\varphi-\beta)\sin\delta}{\cos\varphi\cos\delta\cos\omega + \sin\varphi\sin\delta} \quad (20)$$

where φ is latitude of collector location, δ is declination angle and ω is hour angle.

Furthermore, U_L in "Eq. 16" is collector overall heat loss coefficient and is calculated as follow:

$$U_L = U_t + U_b + U_e \quad (21)$$

where U_t is top loss coefficient, U_b is back loss coefficient and U_e is edge loss coefficient. The top loss coefficient is calculated with "Eq. 22 to 26":

$$U_t = \left(\frac{N}{\frac{C}{T_{pm}} \left[\frac{T_{pm} - T_a}{N+f} \right]^e} + \frac{1}{h_w} \right)^{-1} + \frac{\sigma (T_{pm} + T_a)(T_{pm}^2 + T_a^2)}{\frac{1}{\varepsilon_P + 0.0059 N \cdot h_w} + \frac{2N + f - 1 + 0.133\varepsilon_P}{\varepsilon_g} - N} \quad (22)$$

$$f = \left(1+0.089h_w - 0.1166h_w\varepsilon_p\right)\left(1+0.07866N\right) \quad (23)$$

$$C = 520\left(1-0.000051\beta^2\right) \quad (24)$$

$$e = 0.430\left(1-\frac{100}{T_{pm}}\right) \quad (25)$$

$$h_w = 2.8+3V_w \quad (26)$$

where$N$ is number of glass covers, h_w is wind heat transfer coefficient, V_w is wind velocity and σ is Stefan Boltzmann constant.

Also the back loss coefficient is defined as follow:

$$U_b = \frac{k}{L} \quad (27)$$

Energy efficiency of collector is defined as follow:

$$\eta = \frac{\dot{m}_f \cdot c_P\left(T_{out}-T_{in}\right)-\mathrm{P}_{pump}}{I_T A_c + \mathrm{P}_{agitator}} \quad (28)$$

where$\mathrm{P}_{agitator}$ is power of agitator and in maximum value is about 15 W per every cylindrical obstacle [24]. Also P_{pump} is power of pump and is defined as follow:

$$\mathrm{P}_{pump} = \frac{P_{flow}}{\eta_{pump}\cdot\eta_{motor}} \quad (29)$$

whereη_{pump} and η_{motor} are efficiency of pump and motor, respectively. Also, P_{flow} is dynamic pressure drop of fluid and is calculated as follow:

$$P_{flow} = \frac{\dot{m}_f \cdot \Delta P}{\rho} \quad (30)$$

d) Second law modeling

Exergy is the energy that is available to be used. The rate of exergy equation is defined as follow [25]:

$$\dot{E}_{in} - \dot{E}_{out} - \dot{E}_{loss} - \dot{E}_{des} = \dot{E}_S \quad (31)$$

where$\dot{E}_S$ is rate of storage exergy and with the assumption that the collector operates steady state it is equal to zero. $\dot{E}_{in}$is rate of inlet exergy and includes rate of inlet exergy by inlet fluid to collector ($\dot{E}_{in,f}$) and rate of inlet exergy of absorbed solar radiation ($\dot{E}_{in,Q}$).

The rate of inlet exergy by inlet fluid to collector is defined as follow [25]:

$$\dot{E}_{in,f} = \dot{m}c_p\left(T_{in}-T_a-T_a\ln\left(\frac{T_{in}}{T_a}\right)\right)+\frac{\dot{m}\Delta P_{in}}{\rho} \quad (32)$$

whereΔP_{in} is difference between pressure of inlet fluid and ambient. The rate of inlet exergy of absorbed solar radiation is defined as follow [25]:

$$\dot{E}_{in,Q} = \eta_0 I_T A_c\left(1-\frac{T_a}{T_s}\right) \quad (33)$$

With the assumption that the sun is a black-body, the temperature of it is about 5777 K. According to influence of atmosphere on debilitation of solar radiation, T_s that is called seeming temperature of sun is about 0.75 of sun temperature and is equal to 4333 K approximately [26].

$\dot{E}_{out}$is rate of outlet exergy and includes rate of outlet exergy by exiting fluid of collector ($\dot{E}_{out,f}$) [27].

$$\dot{E}_{out,f} = \dot{m}c_p\left(T_{out}-T_a\ln\left(\frac{T_{out}}{T_a}\right)\right)+\frac{\dot{m}\Delta P_{out}}{\rho} \quad (34)$$

whereΔP_{out} is difference between pressure of outlet fluid and ambient. $\dot{E}_{loss}$is rate of exhausted exergy and includes rate of exhausted exergy from plate to ambient ($\dot{E}_{l,p}$) and exhausted optical exergy ($\dot{E}_{L,optical}$).The rate of exhausted exergy from plate to ambient is defined as follow [28]:

$$\dot{E}_{l,p} = U_L A_c\left(T_{pm}-T_a\right)\left(1-\frac{T_a}{T_{pm}}\right) \quad (35)$$

Because of optical properties of plate, a part of solar radiation does not absorb. Exhausted optical exergy of collector is calculated as follow [29]:

$$\dot{E}_{L,optical} = \frac{\left(1-\eta_0\right)\dot{E}_{in,r}}{\dot{E}_{in,r}} = 1-\eta_0 \quad (36)$$

$\dot{E}_{des}$ is rate of destroyed exergy because of: temperature gradients between plate and sun ($\dot{E}_{d,\Delta Tp\text{-}s}$), temperature gradients between plate and fluid ($\dot{E}_{d,\Delta Tf}$) and pressure drop from inlet to outlet caused by viscosity of fluid, effects of walls of heat sink and also obstacles ($\dot{E}_{d,\Delta P}$). Theses parameters are calculated as follow, respectively [25]:

$$\dot{E}_{d,\Delta T_{p-s}} = \eta_0 I_T A_c T_a\left(\frac{1}{T_p}-\frac{1}{T_s}\right) \quad (37)$$

$$\dot{E}_{d,\Delta T_f} = \dot{m}c_p T_a\ln\left(\frac{T_{out}}{T_{in}}\right)-\dot{m}c_p T_a\frac{T_{out}-T_{in}}{T_p} \quad (38)$$

$$\dot{E}_{d,\Delta p} = \frac{\dot{m}\Delta p T_a\ln\left(\frac{T_{out}}{T_{in}}\right)}{\rho\left(T_{out}-T_{in}\right)} \quad (39)$$

Exergy efficiency of flat-plate solar collector is defined as rate of exergy increasing of fluid in collector to exergy of entering solar radiation to collector and it is calculated as follow [14]:

$$\psi = \frac{\dot{E}_{out,f} - \dot{E}_{in,f}}{I_T A_C \left(1 - \frac{T_a}{T_s}\right) + \mathrm{P}_{agitator}} \quad (40)$$

By combination "Eq. 27 to 36" the exergy efficiency of water-based flat-plate solar collector equipped with stationary and rotational obstacles is achieved.

e) Nanofluid

To calculate the thermophysical properties of nanofluid with spherical nanoparticle, the following equations are proposed. The effective density ρ_{nf} and specific heat $(c_p)_{nf}$ of the nanofluid at the reference temperature (T_a) are determined by the following equations [19]:

$$\rho_{nf} = (1-\phi)\cdot\rho_f + \phi\cdot\rho_{np} \quad (41)$$

$$(c_p)_{nf} = \frac{(1-\phi)(\rho c_p)_{nf} + \phi(\rho c_p)_{np}}{\rho_{nf}} \quad (42)$$

The Patel et al. [31, 32] model supposed to be a general tool to predict the thermal conductivity of CNT-Nanofluids. However, the model is not able to predict well at higher temperature of nanofluids.

$$k_{nf} = k_f \left(1 + \frac{k_{np}\cdot\phi\cdot d_f}{k_f\cdot(1-\phi)\cdot d_{np}}\right) \quad (43)$$

Boboo et al. [33] have proposed the viscosity of MWCNTs-Water correlation based on the experimental data valid up to 1.0% volume concentration.

$$\mu_{nf} = \mu_f \left(1 - 0.50437\phi + 1.744\phi^2\right) \quad (44)$$

f) Validation

A grid independence test was performed for the collector with three rotational obstacles (2 rad/s) at 12 p.m. to analyze the effects of grid sizes on the results. As shown in "Table 3", four sets of mesh are considered and by comparing all mesh configurations, the grid size of 3,728,623 nodes has been adopted to get an acceptable compromise between the computational time and the result accuracy. The computer software validation was done based on the geometry and boundary condition of Khorasanizadeh et al. [2].

In their study the properties of a flat-plate and pipe collector were investigated by empirical measurements. Based on "Fig. 2" it is clear that there is a remarkable coincidence between the empirical [2] and numerical results in the term of outlet temperature of fluid.The maximum error between empirical and numerical results in "Fig. 2" is about 12.5% at time of 9 a.m.

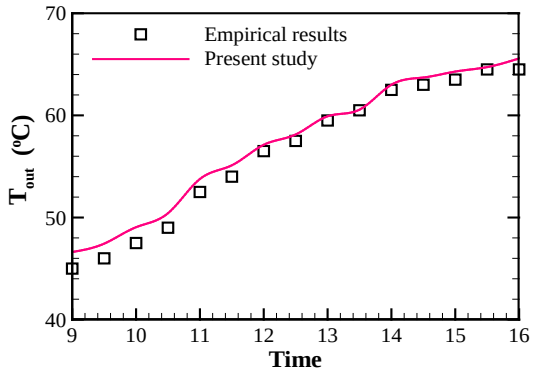

Figure 2: Comparison of the present results with the empirical results of Khorasanizadeh et al. [2], in term of outlet fluid temperature

Table 3: Grid independence test

Nodes	T_{out} (°C)	Error (%)
3,243,983	66.6782	2.22
3,599,007	70.5134	1.05
3,728,623	70.7811	0.02
3,954,131	70.7834	-

III. Results and Discussion

In this section firstly the collector exergy analysis is presented in two different conditions and then the optimization case is investigated.

a) Energy and Exergy Efficiencies

The total heat loss coefficient, mean temperature of absorber plate, collector outlet temperature and energy and exergy efficiencies of simple heat sink (SHS) collector, and heat sink collector equipped with mixers (HSWM) in different hours of day are reported in "Table 4 and 5", respectively. All these values are obtained based on numerical results and analytical correlation. It is realized that energy and exergy efficiencies of SHS collector increase about 30% and 60%, respectively, compared with the reference collector [2] owing to more wetted surface between plate and fluid and more time that it takes the fluid pass the route. Also, the energy efficiency of HSWM increases about 48% in comparison to the reference collector because of the induction of high disturbance and thin boundary layer in the channels equipped with obstacles, leading to higher temperature gradients from inlet to outlet.

On the other side, the exergy efficiency of HSWM increases about 120% compared with the reference collector. Furthermore, the mean temperature of plate and outlet temperature of collector are increasing during the day incessantly because of the collector inlet temperature of fluid that is taken from the reservoir, is constantly increasing due to collector performance in a closed loop and heat saving in the reservoir. Also, in all conditions the inlet radiation flux rate increases from morning to the middle day hours and then decreases. The energy efficiency has the same trend. However, the reason for decreasing the energy efficiency after the afternoon hours is increasing the inlet fluid temperature and also increasing the absorber plate as the time passes that intensifies the losses.

It is clear from "Table 4 and 5" that the $U_L$change in different hours is significant so that in the condition of the collector with simple heat sink the relative difference of U_L at 10 a.m. is about 9% comparing to 16 p.m. This difference is more for other cases. This fact shows that the assumption of constant U_L that some researchers including [30] have considered is not logical and it is necessary to apply its changes in measurements.

Table 4: Results of simple heat sink collector (SHS)

Time	U_L (W/ m²·K)	T_{pm} (°C)	T^o_{ut} (°C)	η (%)	ψ (%)
09:00	7.33	48.11	58.59	54.29	3.34
09:30	7.37	49.06	59.61	57.48	3.53
10:00	7.32	51.32	61.04	57.78	3.95
10:30	7.49	52.41	62.61	64.40	4.21
11:00	7.56	54.25	65.82	63.00	4.35
11:30	7.52	57.07	67.07	63.68	4.58
12:00	7.56	58.42	69.23	61.91	4.60
12:30	7.77	59.31	70.26	61.54	4.55
13:00	7.76	60.46	72.04	61.48	4.54
13:30	7.40	60.57	72.61	60.16	4.68
14:00	7.73	63.22	75.13	58.64	4.67
14:30	7.55	63.47	75.77	57.57	4.56
15:00	7.77	63.89	76.41	56.91	4.41
15:30	7.94	64.09	76.91	56.28	4.21
16:00	7.97	65.11	77.82	55.62	4.15

Table 5: Results of heat sink collector with mixers (HSWM)

Time	U_L (W/ m²·K)	T_{pm} (°C)	T_{out} (°C)	η (%)	ψ (%)
09:00	7.15	47.08	53.23	64.04	6.34
09:30	7.21	48.02	54.24	67.83	6.88
10:00	7.08	50.27	55.51	68.18	7.77
10:30	7.25	51.33	57.49	75.98	8.34
11:00	7.32	53.21	59.61	74.34	8.71
11:30	7.35	56.00	62.29	76.44	9.21
12:00	7.34	57.32	63.71	74.28	9.98
12:30	7.51	58.14	64.40	73.81	8.75
13:00	7.56	59.32	65.87	73.78	8.62
13:30	7.30	59.52	66.01	72.78	8.93
14:00	7.60	62.13	68.82	69.14	8.87
14:30	7.38	62.42	68.99	69.08	8.81
15:00	7.59	62.64	69.11	66.58	8.51
15:30	7.67	63.01	69.25	65.84	8.01
16:00	7.69	64.12	69.34	65.63	7.88

b) Using Nanofluid and Exergetic Optimization

For all two conditions of using the collector, the lowest exergy and energy analysis is related to 9 a.m. either energy efficiency or exergy efficiency are dependent on the I_T and radiation angle. At 9 a.m. the I_T is less and also the angle between the direct sun radiation horizon and vertical to the collector surface is high. Hence the sun radiation absorption is less. In addition, the collector performance due to change in I_T and radiation angle and also the change in temperature of collector inlet water is always transient. These conditions are of high importance in the beginning hours of the day and these are factors of decreasing the efficiency. The effect of changing T_a, I_T, T_{in}, $\eta_0$and $\dot{m}$ parameters on exergy efficiency in different volume fraction of nanoparticles for the optimal condition (HSWM model) in this time was studied to optimize the collector exergically. Therefore, when different values were considered for one parameter, the value at 9 a.m. was assigned to other parameters. The results related to the influence of changing different parameters on the exergy analysis are shown in "Fig. 3 to 7".

In "Fig. 3" the exergy efficiency variation with sun radiation flux for different nanoparticles volume fractions is shown. In the radiation flux changing period, from 300 to 1200 W/m², for all conditions the increasing trend for exergy analysis is observed. By increasing the radiation of sun the temperature of collector outlet fluid increases and this increase leads to exergy efficiency increment.

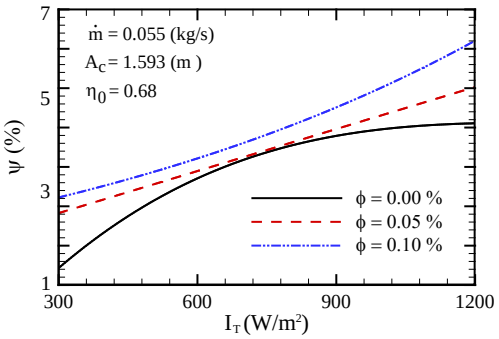

Figure 3: Variation of exergy efficiency of collector with solar radiation for nanifluid in different volume fractions

The exergy efficiency variation with collector inlet fluid temperature for different nanoparticles volume fractions has been demonstrated in "Fig. 4". For base fluid conditions, primarily the exergy efficiency increases until the temperature reaches 65 to 70°C and then it has decreasing trend. On one hand by T_{in} increase, the outlet temperature increases that leads to exergy efficiency increment. On the other hand, T_{in} increase means the fluid temperature inside the collector which raises the thermal loss. So there is one optimum T_{in} that for higher temperatures than it, the effect of exergy efficiency reduction due to higher thermal loss than its increase effect, that is because of fluid outlet temperature increment. But, for nanofluid conditions the exergy efficiency increases by increasing of inlet temperature.

The variation of exergy efficiency with ambient temperature for different nanoparticles volume fractions has been shown in "Fig. 5". For all three conditions of exergy efficiency it has decreasing trend by ambient temperature increase. In this figure the effect of using mixers in exergy efficiency increase due to the heat transfer rate between fluid and collector is perfectly clear.

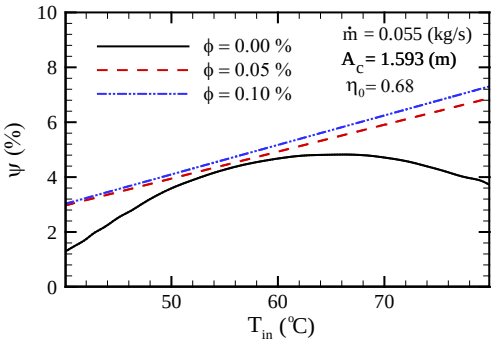

Figure 4: Variation of exergy efficiency of collector with temperature of inlet nanofluid in different volume fractions

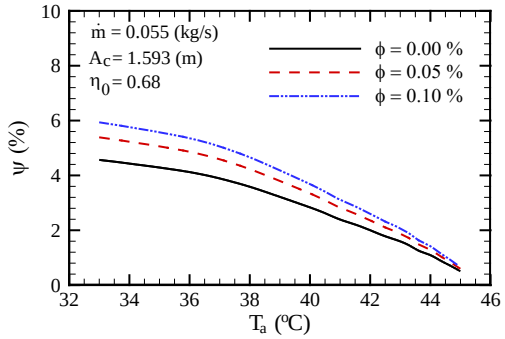

Figure 5: Variation of exergy efficiency of collector using nanofluid in different volume fractions with ambient temperature

In "Fig. 6" the influence of increasing optical efficiency on exergy efficiency for different nanoparticles volume fractions has been demonstrated. By optical efficiency increment for all three collector conditions, the radiation absorption by the absorber plate enhances and causes the fluid temperature inside the collector to increase and therefore the exergy efficiency increases.

In "Fig. 7" the effect of changing the fluid mass flow rate passing through the collector is shown in different nanoparticles volume fractions for mass flow rates from 0.0 to 0.1 kg/s. The applied mass flow rate for three conditions was about 0.055 kg/s. by referring to the results presented in "Fig. 7", it is understood that in the simulations conditions which parameters such as ambient temperature, inlet fluid temperature, optical efficiency, radiate flux and collector cross-section have the same values mentioned in "Table 4 and 5" that are related to 9:00 a.m. For the collector with base fluid, the optimum mass flow rate that causes the exergy efficiency to be maximum, should be ten times lower that means 0.005 kg/s. consequently the exergy efficiency is 5.3% instead of being 4%. Nevertheless, for the condition of using nanofluid the maximum exergy efficiency occurs in the highest mass flow rate of 0.1 kg/s.

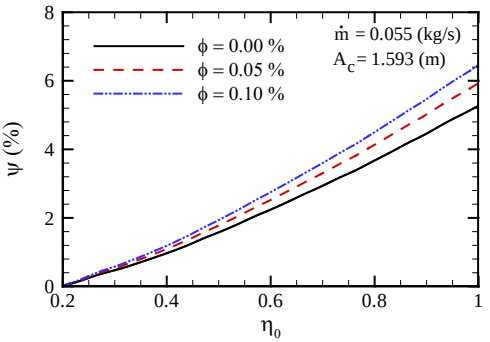

Figure 6: Variation of exergy efficiency of collector with optical efficiency in different nanofluid volume fractions

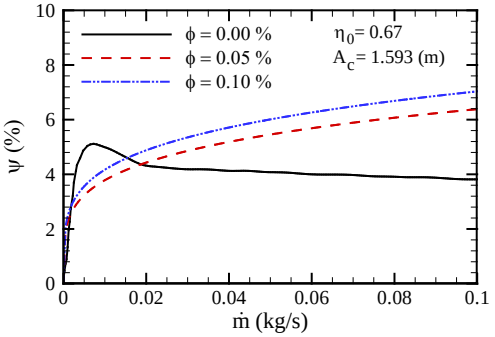

Figure 7: Variation of exergy efficiency of collector with mass flow rate of nanofluid in different volume fractions

IV. Conclusions

Specifying some values of mass flow rate and other parameters that the exergy efficiency get maximum due to them is difficult but in the concept of exergy efficiency, the effect of these parameters is

clearer. In this study, the optimization of a solar collector in a closed circuit for three conditions in the viewpoint of exergy analysis by assuming that U_L is the only variable parameter and the fluid temperature is not equal to ambient temperature. The effect of using the mixers and nanofluid through fluid passage was studied and these results were obtained:

- Solar radiation flux increase and optical efficiency increase lead to exergy efficiency increase for all conditions.
- The exergy efficiency decrease by ambient temperature increase but by increasing the collector inlet fluid temperature the exergy efficiency increases to the certain temperature and then decreases. But, by using nanofluid the exergy efficiency always increases by increasing inlet temperature.
- For each special collector there is unique mass flow rate that the exergy efficiency gets maximum. For higher mass flow rates of base fluid, primarily the efficiency slightly decreases and then remains unchanged. But, by using nanofluid the maximum exergy efficiency occurs in the highest mass flow rate.
- Generally, using mixers and nanofluid enhance the exergy efficiency. In fact, while the trend of exergy efficiency variation with effective parameters is increasing, applying the obstaclesprecipitate the efficiency increment.in addition for the case that the trend of exergy efficiency variation with changing these parameters is decreasing, the decreasing trend gets slow.
- The collector performance in a closed circuit causes the collector inlet fluid temperature to increase constantly in the condition that the reservoir temperature increases due to not using the stored heat in it. The temperature increase leads to exergy efficiency increase to a certain point and then decreases this efficiency for higher values.

Nomenclature

A	area (mm^2)
B	slop (deg)
c_p	specific heat capacity (J/kg·K)
D	diameter (mm)
$\dot{E}$	energy rate (kW)
H	height (mm)
I	irradiation (W/m^2)
k	thermal Conductivity (W/m·K)
L	length (m)
$\dot{m}$	mass flow rate (kg/s)
N	number of glass covers
n_o	numberof mixers
P	pressure (Pa)
P	power (W)
Pr	Prandtlnumber
R	ratio of beam radiation
S	solar radiation per plate area unit (W/m^2)
T	temperature (°C)
U	heat loss coefficient ($W/m^2 \cdot K$)
u	velocity (m/s)
V	velocity(m/s)
W	width (mm)
x	axial direction

Greek symbols

α	absorption coefficient
β	slop (deg)
δ	thickness (mm)
δ	desalination angle (deg)
ε	emissivity coefficient
η	energy efficiency
η_o	optical efficiency
μ	dynamic viscosity ($N \cdot s/m^2$)
ρ	density (kg/m^3)
σ	Stefan Boltzmann constant
τ	transmissioncoefficient
φ	volume fraction
ϕ	latitude of collector location
ψ	exergetic efficiency
ω	hour angle (deg)

Subscripts

a	ambiaent
c	collector
e	exit of heat sink
f	base fluid
fo	first mixer
g	glass cover
i	inlet to heat sink
in	inlet
ins	insulator
m	mean
nf	nanofluid
np	nanoparticle
o	mixer (obstacle or agitator)
p	absorber plate
T	tilted surface
t	transient
w	wind

References Références Referencias

1. Kalogirou, S.A., 2004. "Solar thermal collectors and applications". *Progress in Energy and Combustion Science*, 30(3), pp. 31-95.
2. Khorasanizadeh, H.,Aghaei, A., Ehteram, H., and Azimi, A., 2013. "Study and Exergy Optimization of a Flat Plate Solar Collector in a Closed Circuit Utilized with Reflectors and Lenses Using Experimental Results". *Journal of Energy Engineering Management*, 3(1), pp. 40-51.
3. Leon, M.A., and Kumar, S., 2007. "Mathematical modeling and thermal performance analysis of

unglazed transpired solar collectors", *Solar Energy*, 81, pp. 62-75.
4. Motahar, S., and Alemrajabi, A.A., 2010. "An analysis of unglazed transpired solar collectors based on exergetic performance criteria". *International Journal of Thermodynamics*, 13(4), pp. 153-160.
5. Kutscher, C.F., Christensen, C.B., and Barker, G.M., 1993. "Unglazed transpired solar collectors: heat loss theory", *Journal of Solar Energy Engineering*, 115, pp. 182-188.
6. Yildiz, C., Torgrul, I.T., Sarsilmaz, C., and Pehlivan, D., 2002. "Thermal efficiency of an air solar collector with extended absorption surface and increased convection", *International Communication in Heat and Mass Transfer*, 29(6), pp. 831-840.
7. Tsilingiris, P.T., 2000. "Heat transfer analysis of low thermal conductivity solar energy absorbers", *Applied Thermal Engineering*, 20, pp. 1297-1314.
8. Khattab, N.M., 2000. "Evaluation of perforated plate solar air heater", *International Journal of Solar Energy*, 21, pp. 45-62.
9. Njomo, D., and Daguenet, M., 2006. "Sensitivity analysis of thermal performances of flat plate solar air heaters", *Heat and Mass Transfer*, 42, pp. 1065-1081.
10. Sarreshtedari, A., and ZamaniAghaee, A., 2014. "Investigation of the thermo-hydraulic behavior of the fluid flow over a square ribbed channel", *Journal of Heat and Mass Transfer Research*, 1(2), 101-106.
11. Baniamerian, Z. Mehdipour, R. and Kargar, F., 2015. "A numerical investigation on aerodynamic coefficients of solar troughs considering terrain effects and vortex shedding", *International Journal of Engineering (IJE), Transactions C: Aspects*, 28(6), pp. 940-948.
12. Ziapour, B.M., and Rahimi, F., 2016. "Numerical study of natural convection heat transfer in a horizontal wavy absorber solar collector based on the second law analysis", *International Journal of Engineering (IJE), Transactions A: Basics*, 29(1), pp. 109-117.
13. Ajay, K., and Kundan, L., 2016. "Performance evaluation of nanofluid (Al2O3/H2O-C2H6O2) based parabolic solar collector using both experimental and CFD techniques", *International Journal of Engineering (IJE), Transactions A: Basics*, 29(4), pp. 572-580.
14. Luminosu, I., and Fara, L., 2005. "Determination of the optimal operation mode of a flat solar collector by exergetic analysis and numerical simulation", *Energy*, 30(12), pp. 731-747.
15. Shojaeizadeh, E., and Veysi, F., 2016. "Development of a correlation for parameter controlling using exergy efficiency optimization of an Al_2O_3/water nanofluid based flat-plate solar collector", *Applied Thermal Engineering*, 98, pp. 1116-1129.
16. Said, Z. Saidur, R. and Rahim, N.A., 2016. "Energy and exergy analysis of a flat plate solar collector using different sizes of aluminium oxide based nanofluid", *Journal of Cleaner Production*, 133, pp. 518-530.
17. Mollamahdi, M. Abbaszadeh, M. Sheikhzadh, GH.A., 2016."Flow field and heat transfer in a channel with a permeable wall filled with Al_2O_3-Cu/water micropolar hybrid nanofluid, effects of chemical reaction and magnetic field", *Journal of Heat and Mass Transfer Research*, 3(2), pp. 101-114.
18. Hemmat Esfe, M. Seedodin, S., 2016. "Numerical investigation of combined convection flow in a cavity subjected to a nanofluid with an inside hot obstacle: effect of diameter of nanoparticles and cavity inclination angles", *Journal of Heat and Mass Transfer Research*, Articles in Press.
19. Vanaki, Sh.M. Mohammed, H.A. Abdollahi, A. and Wahid, M.A., 2014. "Effect of nanoparticle shapes on the heat transfer enhancement in a wavy channel with different phase shifts", *Journal of Molecular Liquids*, 196, pp. 32-42.
20. Gray, D.D., and Giorgini, A., 1976. "The validity of the Boussinesq approximation for liquids and gases", *International Journal of Heat and Mass Transfer*, 19(5), pp. 545-551.
21. Bejan, A., 1984. "Convection heat transfer", *Wiley-Interscience*.
22. ANSYS Fluent-Solver Theory Guide, Release 14.0, 2011, pp. 351-353.
23. Duffie, J.A., and Beckman, W.A., 2006. "Solar engineering of thermal processes", New York, John Wiley & Son.
24. Mechanical Agitator Power Requirements for Liquid, www.pdhonline.com/courses/k103/k103content.pdf
25. Suzuki, A., 1988. "General theory of exergy balance analysis and application to solar collectors", *Energy*, 13(2), pp. 123-160.
26. Bejan, A., Keary, D.W., and Kreith, F., 1981. "Second law analysis and synthesis of solar collector systems", *Journal of Solar Energy Engineering*, 103(1), pp. 23-28.
27. Bejan, A., 1988. "Advanced Engineering Thermo-dynamics", New York, Wiley Inter science.
28. Dutta Gupta, K.K. and Saha, S., 1990 "Energy analysis of solar thermal collectors", *Renewable energy and environment*, 33(1), pp. 283-287.
29. Kahrobaian, A., and Malekmohammadi, H., 2008. "Exergy optimization applied to linear parabolic solar collectors", *Journal of Faculty of Engineering*, 42(1), pp. 131-144.
30. Farahat, S., Sarhaddi, F., and Ajam, H., 2009. "Exergetic Optimization of Flat Plate

SolarCollectors", *Renewable Energy*, 34(4), pp. 1169 -1174.
31. Patel, H.E., Anoop, K.B., Sundararajan, T., and Das, S., 2008, "Model for thermal conductivity of CNT-nanofluids", *Bulletin of Materials Science*, 31(3), pp. 387–390.
32. Kumaresan, V., and Velraj, R., 2012 "Experimental investigation of the thermo-physical properties of water–ethylene glycol mixture based CNT nanofluids", *Thermochim. Acta*, 545, pp. 180–186.
33. Bobbo, S., Fedele, L., Benetti, A., Colla, L., Fabrizio, M., and Pagura, C., 2012 "Viscosity of water based SWCNH and TiO2 nanofluids", *Experimental Thermal and Fluid Science*, 36, pp. 65–71.

This page is intentionally left blank